2012 International Conference on Industrial and Intelligent Information (ICIII 2012)
IPCSIT vol.31 (2012) © (2012) IACSIT Press, Singapore

Three-Dimensional Morphology Quantification of Biofilm Structures from Confocal Laser Scanning Microscopy Images

Jerzy S. Zielinski[1], Agnieszka K. Zielinska[2], Nidhal Bouaynaya[1]

[1] University of Arkansas in Little Rock

[2] University of Arkansas for Medical Sciences

Abstract. Staphylococcus aureus is an opportunistic human pathogen and a causative agent of a wide range of diseases. Its hallmark feature is a capability to form biological structures called biofilms, in which bacteria can embed themselves in a protective matrix. The study of biofilm structures and morphologies is central to understand the biological characteristics of the biofilm including its resistance to drugs. These studies, however, have focused on two-dimensional (2D) analysis of the biofilm images. In this paper, we show the importance of three-dimensional analysis of the biofilm morphology by taking into account the temporal information between the images. Specifically, we show that the morphological features computed from a simple gradient-based three-dimensional segmentation method outperforms not only its 2D homologue but also sophisticated two-dimensional segmentation methods like the watershed algorithm. Our analysis is applied to real biofilm confocal laser scanning microsopy images with a ground truth delineated manually by expert biologists at the University of Arkansas for Medical Sciences.

Keywords: Staphylococcus aureus, Confocal Laser Scanning Microscopy, three-dimensional segmentation.

1. Introduction

Staphylococcus aureus is an opportunistic human pathogen responsible for diseases that vary in clinical presentation and severity, ranging from minor skin infections to life-threatening conditions such as pneumonia, endocarditis and toxic shock syndrome. Increasing rates of staphylococcal infections combined with dramatic increase of number of infections caused by multi-antibiotic resistant strains led to the situation in which MRSA (methicillin-resistant *S. aureus*) mortality rates surpassed those of HIV in the USA (Nygaard rt al., 2008). For that reason, there is a strong need to understand pathogenesis of Staphylococcus aureus infections. Studies have shown that there are two major elements contributing to the fact that these life-threatening infections are so difficult to treat. The first is the emergence of new antibiotic-resistant strains and the second is that many *S. aureus* infections are associated with the formation of a biofilm, which limits the efficacy of any antimicrobial therapy. Biofilms shield microorganisms from stressful environmental conditions including the defensive mechanisms of the host immune system and antimicrobials. Since biofilm formation is such a detrimental element of *S. aureus* infection, it requires extensive studies. One of the most important parameters of biofilm that is used in biological studies is the area occupied by the biomass, i.e. biomass volume. Due to the fact that the biofilm is a porous structure, in order to compute biomass volume, it is necessary to differentiate the area occupied by the biofilm from the surrounding noisy background.

One of the most comprehensive imaging techniques used for the assessment of the biofilm structure is the confocal laser scanning microscopy (Lawrence et al., 2002). By using several fluorescent stains or conjugated antibodies in combination with multichannel CLSM 3D, the location of different biofilm constituents can be recorded. The majority of confocal laser scanning microscopy (CLSM) image quantification methodologies require regionsegmentation, i.e. the identification of similar regions and the

differentiation of the signal of interest in the image from the background. There are several methods described in the literature, which target the problem of biological structure recognition from CLSM images. Most of these methods, however, rely on a two dimensional segmentation of the images in order to extract morphological features of the biofilm (Zielinski at al., 2011). Sima et al. presented an automatic segmentation of small 3D objects using multiscale wavelet edge detection method, where edges are detected by filtering the image with low-pass filters of different sizes followed by an application of the gradient operator. This method, although 3D, is suitable for branch-like structures like neurons, but fails in the recognition of the more irregular and compact shapes formed by biofilms. In this paper, we perform 3D Biofilm Morphology Quantification.

The three dimensional morphology of biofilms can be quantified using volumetric parameters, which are calculated from voxels in the 3D structure of the biofilm. In this paper, we use the average run lengths (in *X*, *Y* and *Z* direction), the aspect ratio, the average and maximum diffusion distances (Haluk et al., 2004), biomass and average thickness as important clinical features of the biofilm.

1.1. Average Run Length

The run length measures the number of consecutive cluster pixels in a given direction, and an average run length measures the average length of consecutive cluster pixels in the measurement direction. For instance, if a biofilm has a large average X-run length and a small average Y-run length, then the biofilm appears stretched in the X direction. This may indicate special growth patterns of the biofilm (Haluk et al., 2004)

1.2. Aspect Ratio

The aspect ratio is defined as the ratio of the average X-run length to the average Y-run length along the Y-axis. It indicates the symmetry of growth in the X and Y directions. In particular, significant variation of the aspect ratio may indicate the presence of stress or micro-colonies that affect the normal growth of the biofilm (Haluk et al.,2004)

$$Aspect\ Ratio = \frac{Average\ Run\ Lenth\ X}{Average\ Run\ Lenth\ Y}$$

1.3. Average and Maximum Diffusion Distance

The diffusion distance is the minimum linear distance from a cluster voxel to the nearest void voxel in a three-dimensional structure. The average diffusion distance is the average of all diffusion distances. The maximum diffusion distance is defined as the distance to the most remote pixel in the cell cluster from a void cluster. (Haluk et al., 2004). Biologically, the diffusion distance indicates the distance over which the biofilm has to diffuse in the cell structure.

1.4. Biomass

The biomass in bio-volume, V, is measured from numeric integration of the area of microbial colonization profiles, following a method previously described in (Keuhn et al.,1998)

$$V = \int S(z)dz \approx \left[\frac{1}{2} \times S(z_1) + \sum_{m=2}^{m_e} S(z_m) + \frac{1}{2} \times S(z_{m_e}) \right] \times \Delta z$$

1.5. Average Thickness

The average thickness of the biofilm is calculated as the average value of the height of all clusters of the biofilm rise from solid-substratum in the z direction between cross-sections.

Three-Dimensional Segmentation is the accurate segmentation of highly porous objects from a noisy background, e.g., bacterial cells in a biofilm from the medium, is a challenging task in image processing. We show that a simple three-dimensional (3D) segmentation, which relies on the 3D gradient, outperforms the status-quo two-dimensional segmentation techniques used for the delineation of biofilms (Zielinski et al., 2011). The power of 3D segmentation stems from the fact that it takes into account the temporal correlation in addition to the spatial correlation accounted for in 2D analysis.

The gradient field finds edges in the image by treating the set of image as a 3D surface or a video. The 3D region recognition and image segmentation follows this simple two-threshold level procedure:

1. Compute the 3D gradient field on volume created by stacking CLSM images as follows:

$$\nabla F = \frac{\partial F}{\partial x}\hat{l} + \frac{\partial F}{\partial y}\hat{J} + \frac{\partial F}{\partial z}\hat{k}$$

where F denotes the 3D image surface or the set of 2D images.

2. Threshold the gradient magnitude in order to find the boundaries of 3D structures buried in the noisy background.

3. Compute the arithmetic mean of intensity of the obtained binary image surface in order to refine the threshold level.

4. Threshold the volume into binary values based on the calculated level of refined threshold.

2. Application to CLSM Biofilm Images

2.1. Biofilm culture preparation and image acquisition

Costar 3596 plates (Corning Life Sciences, Acton, MA) wells were coated overnight at 4^{o}C with 20% human plasma (Sigma) in bicarbonate buffer. Overnight cultures of *S. aureus* grown in biofiolm media (TSB-NaCl/Glc) were diluted to an OD_{600} of 0.05 in fresh TSB-NaCl/Glc. After removing human plasma, 200 ul of each culture was transferred to wells and incubated for 24 h at 37^{o}C. The next day, the wells were gently washed three times with 0.85% (wt/vol) NaCl, followed by staining with mixture of SYTO-9 and propidium iodide diluted in 0.85% (wt/vol) NaCl (Cat\# L7012; Invitrogen, Carlsbad, CA) for 18min. After removing the stain, the wells were gently washed once with 0.85% (wt/vol) NaCl. Biofilm images were collected by CLSM using a LSM 510 META confocal scanning system (Zeiss, Thornwood, NY) and Axiovert 200 motorized inverted microscope (Zeiss). SYTO 9 (green, live cells) fluorescence was detected by excitation at 488 nm, and emission was collected with a 500- to 530-nm bandpass filter. Propidium Iodide (red; dead cells) fluorescence was detected by excitation at 488 nm and emission was collected with a 565-615 nm bandpass filter. All z-sections were collected at 1- um intervals by using a C-Apochromat 40x/1.2W H_2O objective lens. Image acquisition and processing was performed by using an LSM Image Browser (Zeiss).

2.2. Segmentation and parameter quantification results

Z-stack Confocal Scanning Microscopy Images of three different *S. aureus* colonies were processed using 2D segmentation and 3D segmentation methods separately. The expert biologist, Agnieszka Zielinska, performed a (tedious) manual segmentation of the biofilm to be used as the ground truth. The segmentation and parameter quantification results of 3D and 2D methods are assessed using the mean square error criterion. Figure 1 shows the output of the 2D and 3D segmentations of a stack of CLSM images. It is clear that the 3D segmentation better captures the biofilm surface than its 2D homologue. Figures 2 and 3 further shows the mean square error of the 2D gradient-based segmentation, the 2D watershed segmentation (Zielinski at al., 2011 and Meyer et al., 1994), and the 3D gradient-based segmentation. For all the images we had in our dataset, the error was significantly smaller in 3D segmentation than in 2D segmentation. We, therefore, expect that the resulting 3D biofilm quantification parameters are more accurate than their corresponding 2D values. Indeed, this is confirmed by the results displayed in Tables 1, 2 and 3 for the biofilm parameters: average run length, aspect ratio, average and maximum diffusions, biomass and average thickness. Amazingly, the simple 3D gradient-based segmentation not only performs better than the 2D gradient-based segmentation but also shows a higher performance, in terms of mean square error, than the sophisticated 2D watershed segmentation.

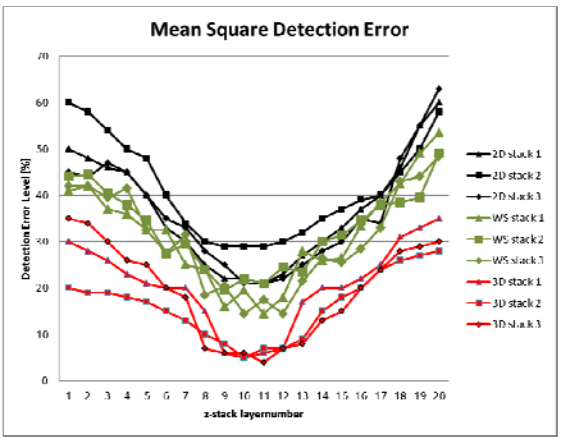

Figure 2 Mean Square Error of 2D gradient-based segmentation (black), 2D watershed segmentation (green) and 3D (red) gradient-based segmentation applied to CLAS z-stack of images.

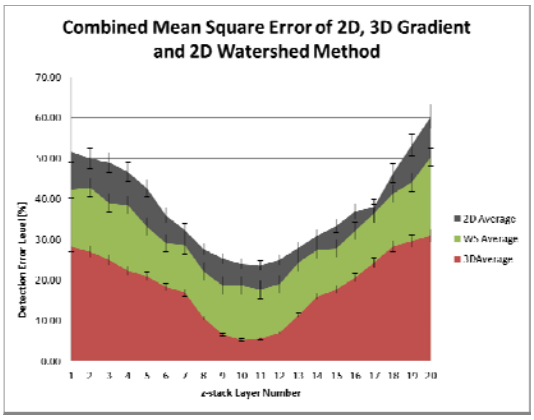

Figure 3. Combined Mean Square Error of 2D gradient-based (black), 2D watershed (green) and and 3D gradient-based segmentations.

Table 1: Results of biofilm parameter quantification for Stack 1 for 3D and 2D segmentations in comparison with the ground truth.

	Ground Truth	3D- gradient segmentation	2D-gradient segmentation	2D Watershed segmentation
Average Run Length X [um]	12.98	12.45	9.69	12.00
Average Run Length Y [um]	12.47	11.65	9.28	11.10
Average Run Length Z [um]	5.02	4.98	4.20	4.56
Aspect Ratio	1.04	1.06	1.04	1.08
Average Diffusion Distance [um]	3.25	2.56	1.30	2.52
Maximum Diffusion Distance [um]	15.70	15.69	13.20	14.98
Biomass [um^3/um^2]	5.03	4.87	4.56	4.72
Average Thickness [um]	10.47	9.25	8.98	9.02

Table 2: Results of biofilm parameter quantification for stack 2 for 3D and 2D segmentations in comparison with the ground truth.

	Ground Truth	3D-gradient segmentation	2D-gradient segmentation	2D Watershed segmentation
Average Run Length X [um]	21.32	20.75	19.69	20.09
Average Run Length Y [um]	20.50	20.67	19.38	20.01
Average Run Length Z [um]	6.02	6.98	6.20	6.50
Aspect Ratio	1.04	1.00	1.01	1
Average Diffusion Distance [um]	4.40	4.66	4.30	4.40
Maximum Diffusion Distance [um]	15.96	15.99	15.64	15.70
Biomass [um^3/um^2]	7.59	6.97	5.71	6.30
Average Thickness [um]	12.53	11.38	10.00	11.00

Table 3: Results of biofilm parameter quantification for stack 3 for 3D and 2D segmentations in comparison with the ground truth.

	Ground Truth	3D-gradient segmentation	2D-gradient segmentation	2D Watershed segmentation
Average Run Length X [um]	52.98	50.48	48.00	49.86
Average Run Length Y [um]	50.47	48.93	47.14	48.21
Average Run Length Z [um]	14.02	14.06	13.04	13.85
Aspect Ratio	1.05	1.03	1.02	1.03
Average Diffusion Distance [um]	10.25	9.37	9.10	9.20
Maximum Diffusion Distance [um]	55.70	15.69	13.20	14.97
Biomass [um^3/um^2]	20.65	19.65	18.91	19.03
Average Thickness [um]	24.56	24.00	23.46	23.92

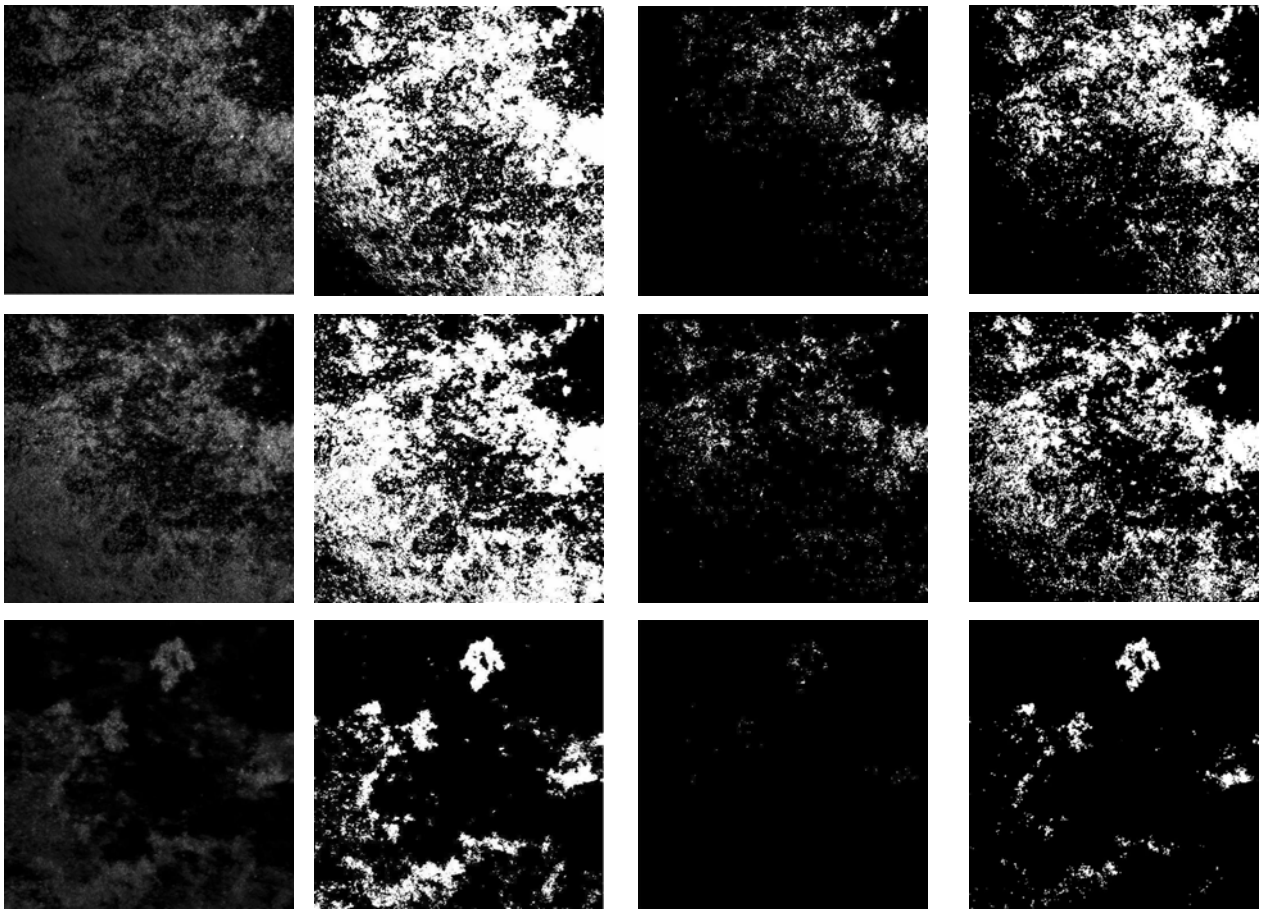

Figure 1. 2D and 3D-gradient based segmentation: Column 1: the original CLSM images. Column 2: 3D gradient-based segmentation; Column 3: 2D gradient-based segmentation; Column 4: 2D Watershed Segmentation

3. Conclusion

In this paper, we showed the importance of 3D analysis of biofilm structures, which yields more accurate morphological parameter quantification for clinical and biological assessment of the biofilm than sophisticated 2D-based analysis like the watershed segmentation. Two-dimensional analysis of the biofilm morphology treats the CLSM images independently from each other, whereas the 3D analysis takes into account the temporal correlation between the stacked images. Even though the proposed 3D segmentation relies on a simple 3D gradient computation, we showed that the resulting biofilm parameters are more accurate than sophisticated 2D-based segmentations, like the watershed segmentation. Accurate computation of biofilm morphological parameters, like biomass, thickness and diffusion coefficients, are pivotal to understanding biofilm growth and biological characteristics; and thus design efficient therapeutics to target it.

4. References

[1] Boothby, William; An introduction to differentiable manifolds and Riemannian geometry. Pure and Applied Mathematics, volume 120 (second ed.). Orlando, FL: Academic Press (1986). ISBN 0-12-116053-X

[2] Haluk Beyenal, Conrad Donovan, Zbigniew Lewandowski, Gary Harkin; Three-dimensional biofilm structure quantification Journal of Microbiological Methods 59 (2004) 395– 413

[3] Heydorn A; Nielsen AT; Hentzer M; Sternberg C; Givskov M; Ersbll BK; Molin S., "Quantification of biofilm structures by the novel computer program comstat.," Microbiology, vol. 146, pp. 2395–2407, 2000.

[4] Hubbard, J. H.; Hubbard, B. B.. Vector calculus, linear algebra, and differential forms. A unified approach. Upper Saddle River, NJ (1999): Prentice Hall. ISBN 0-13-657446-7

[5] Lawrence JR; Neu TR; Marshall KC, Colonization, adhesion, aggregation and biofilms, American Society for Microbiology, 2002.

[6] Kuehn M; Hausner M; Bungartz HJ, Wagner M; Wilderer PA; Wuertz S, "Automated confocal laser scanning microscopy and semiautomated image processing for analysis of biofilms.," Applied and Environmental Microbiology, vol. 64, no. 11, pp. 4115–4127, 1998.

[7] Meyer; Fernand, "Topographic distance and watershed lines.," Signal Processing, vol. 38, pp. 113–125, 1994.

[8] Nygaard TK; DeLeo FR; Voyich JM, "Community-associated methicillin resistant staphylococcus aureus skin infections: advances toward identifying the key virulence factors.," Curr Opin Infect Dis, vol. 21, no. 2, pp. 147–152, 2008.

[9] Rice KC; Mann EE; Endres JL; Weiss EC; Cassat JE; Smeltzer MS; Bayles KW, "The cida murein hydrolase regulator contributes to dna release and biofilm development in staphylococcus aureus.," Proceedings of the National Academy of Sciences of the United States of America, vol. 104, no. 19, pp. 8112–8118, 2007.

[10] Sharpe, R. Differential geometry. Springer-Verlag (1997). ISBN 0-387-94732-9

[11] Staudt C; Horn H; Hempel DC; Neu TR., "Volumetric measurements of bacterial cells and extracellular polymeric substance glycoconjugates in biofilms.," Biotechnol Bioeng., vol. 88, no. 5, pp. 585–592, 2004.

[12] Xavier J.B.; White D.C. ; Almeida J.C., "Automated biofilm morphology quantification from confocal laser scanning microscopy imaging.," Water Science and Technology, vol. 47, no. 5, pp. 31–37, 2003.

[13] Zielinski J.S., Zielinska A.K., Bouaynaya N, Smeltzer M.S. "Automated Biofilm Region Recognition And Morphology Quantification From Confocal Laser Scanning Microscopy Imaging", in Biomedical Science and Engineering Conference - Image Informatics and Analytics in Biomedicine (BSEC 2011), Knoxville, Tennessee, March 2011.